NiAl Underlayers For CoCrTa Magnetic Thin Films

Li-Lien Lee, David E. Laughlin and David N. Lambeth*

Department of Materials Science and Engineering, *Department of Electrical and Computer Engineering,
Data Storage Systems Center, Carnegie Mellon University, Pittsburgh, PA 15213

Abstract -- CoCrTa films were sputter-deposited on either NiAl or Cr underlayers on glass substrates and their coercivities were compared. The NiAl film was found to have the B2 structure with a lattice parameter of ~0.288nm. The grain size of a 100nm NiAl film is ~15nm, which is about 50% smaller than a similarly deposited Cr film. As the CoCrTa/Cr films the CoCrTa/NiAl films show a similar increase of the in-plane coercivity with thickening of the underlayer. X-ray diffraction studies showed that CoCrTa/NiAl films have a stronger $(10\bar{1}0)$ peak than CoCrTa/Cr films. Substrate heating and biasing during deposition of the NiAl underlayer are less helpful than in the case of Cr underlayer.

I. INTRODUCTION

Important magnetic properties, such as the coercivity (Hc), remanent magnetization (Mr) and coercive squareness (S*), which are crucial to the storage performance of the Co alloy magnetic thin film depend primarily upon the microstructure of the media. To achieve the 10 Gb/in^2 goal of the rigid disk drive industry, further improvement of the thin film's microstructure is needed. It is generally recognized that the microstructure of a high density longitudinal recording Co alloy thin film needs 1) a crystallographic texture in which the crystalline c-axis lies in the plane of the film 2) uniform small grains with grain boundaries which can magnetically isolate neighboring grains [1]-[5]. Other than by the right choice of the Co alloy and fine tuning of the deposition process, the desired thin film microstructure can also be acquired through the proper use of an underlayer.

Many different underlayer materials for longitudinal media , such as Cr, Mo, W, Ti, NiP, CrV and Cr alloyed with other substitutional elements, have been reported in the literature [6]-[11]. Only a few of these, however, actually perform well. Among them, the most often used and the most successful underlayer is pure Cr. It has been shown [12] that BCC Cr underlayers promote grain-to-grain epitaxial growth of HCP Co alloy thin films deposited on these underlayers. The microstructure of small grains with in-plane c-axis texture and marked improvement of magnetic properties are observed in Co alloy films with Cr underlayers.

Here we report on an entirely different underlayer material, an ordered alloy, for the use as an underlayer. Its microstructure appears to provide potential benefits over the Cr underlayer.

NiAl Underlayer

NiAl is a Hume-Rothery β-phase electron compound with a valence electron/atom ratio of 3/2, which gives rise to a B2 crystal structure up to its congruent melting point of 1911K. For bulk samples, the superlattice is stable over a wide composition range from 41.5 to 55 at% Al at 400°C [13]. B2 is an ordered structural derivative of the BCC structure, the structure of Cr. Schematics of the crystal structures of NiAl and Cr are shown in Fig. 1. Notice that NiAl has an almost identical lattice constant as Cr, 0.288nm [14].

From the epitaxy point of view, the NiAl underlayer and the Cr underlayer should provide a similar texture control of the Co alloy film. NiAl forms a highly stable B2 ordered phase because of the strong bonding between the Ni and Al atoms. This implies low atomic mobility which in turn can yield a smaller grain size. In addition, NiAl is paramagnetic with a very low susceptibility [15] and has good thermal conductivity, high stiffness and good environmental corrosion resistance. It is reasonable to think that NiAl could be a good candidate for the substitution of the Cr underlayer.

II. EXPERIMENTAL

Thin films of $Co_{86}Cr_{12}Ta_2$/Cr, $Co_{86}Cr_{12}Ta_2$/NiAl, Cr and NiAl were deposited on glass substrates by RF diode sputtering in a LH Z-400 sputtering system. The base pressure was 5×10^{-7} Torr or lower and the sputtering pressure of the Ar gas was 10 mTorr. Sputtering was performed at a fixed AC power of 2.3 W/cm^2 at various substrate bias and heating conditions. The magnetic layer, CoCrTa, was maintained at a constant thickness of 40nm for all the samples by controlling the pre-calibrated deposition time. Film microstructures were studied by transmission electron microscopy (TEM), energy dispersive x-ray spectroscopy
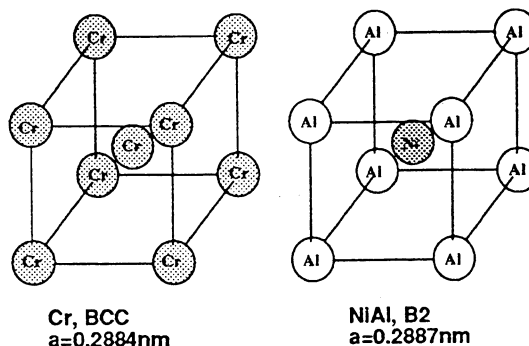

Cr, BCC
a=0.2884nm

NiAl, B2
a=0.2887nm

Fig. 1. Crystal structures of the Cr (BCC) and NiAl (B2).

(EDX), and by X-ray diffractometry with Cu K_α radiation. The in-plane magnetic properties of the thin films were measured by vibrating sample magnetometry (VSM) with fields up to 10 kOe.

III. RESULTS AND DISCUSSION

Fig. 2 shows the TEM diffraction ring patterns of 100nm thickness NiAl and Cr films sputter-deposited without substrate bias or heating. The superlattice reflection rings indicate that the NiAl film is indeed the B2 ordered structure, and judging from the well matched fundamental rings its lattice constant is very close to that of the Cr. The plane view micrograph of a 100nm NiAl film deposited on glass, Fig. 3, shows equiaxed grains with an average grain size of ~15nm which is about 50% smaller than the grain size of a similarly deposited Cr film [16]. A uniform, fine grain underlayer is always beneficial because it renders the possibility of a finer grain Co film. Whether the Co film can inherit the fine grain and still have good recording properties will be studied in our future work. The EDX analysis of the NiAl film shows its composition is 52.3 at% Al and 47.7 at% Ni which is well within the B2 phase region of the Al-Ni phase diagram [13].

Fig. 4 shows the coercivity values of 40nm thick CoCrTa films deposited on various thicknesses of NiAl or Cr underlayers without substrate bias or heating. In both cases, the coercivity increases and then reaches a plateau as the underlayer thickens. The CoCrTa/NiAl films have higher Hc except when the underlayer is thinner than 100nm. Fig. 5 is similar to Fig. 4 except the CoCrTa layer was deposited at a -200V substrate bias. The substrate bias increases Hc in both the CoCrTa/Cr and CoCrTa/NiAl films. But the Hc increase in CoCrTa/Cr films is higher. X-ray diffraction studies showed that the Cr underlayer has a stronger {110} texture than the NiAl underlayer, see Fig. 6. At the same time the CoCrTa films prepared on NiAl underlayers have a stronger {10$\bar{1}$0} texture. Our studies show that as the underlayer thickness increases the {112} x-ray peak appeared in the NiAl film earlier than in the Cr film. Therefore we believe

that the {10$\bar{1}$0} of CoCrTa is heteroepitaxially grown on the {112} of NiAl. There is no observable {10$\bar{1}$1} peak in the CoCrTa/NiAl film.

It has been reported that substrate bias during the Cr sputtering process alone can increase the Hc of the CoCrTa/Cr film by about 60% [17]. Similarly, we applied bias during the NiAl deposition of CoCrTa/NiAl films. However, we found that substrate bias during NiAl sputtering decreased the coercivity of the CoCrTa/NiAl film, Fig. 7. Our EDX analysis showed that bias sputtering changed the composition of the NiAl film. An increase of substrate bias voltage from 0 to -200V can change the Al content from 52.3 at% to 42.9 at%. This is due to the preferential resputtering of the Al during the deposition. The TEM diffraction ring pattern of a -200V substrate bias sputtered NiAl film shows rings belonging to a mixture of B2 NiAl and the orthorhombic Ni_5Al_3 phases. While this Ni_5Al_3 phase would not be anticipated for equilibrium bulk samples the sputtered thin film is probably not at equilibrium. As the bias voltage was increased the CoCrTa film gradually lost its epitaxially grown {10$\bar{1}$0} texture, and as a result its coercivity decreased. In the future, we will compensate for this composition shift by adjusting the target composition.
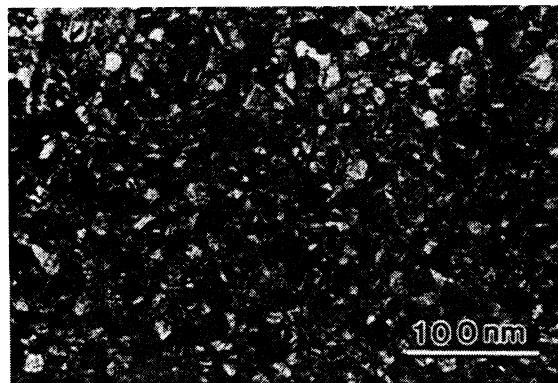
From Fig. 8, we see that the Hc of CoCrTa/NiAl films

Fig. 3. Bright field TEM micrograph of a RF sputtered 100nm NiAl film. The grain size is ~15nm.

Fig. 4. Coercivity vs. underlayer thickness of a 40nm CoCrTa film sputter-deposited without substrate bias. NiAl and Cr underlayers were also deposited without bias.
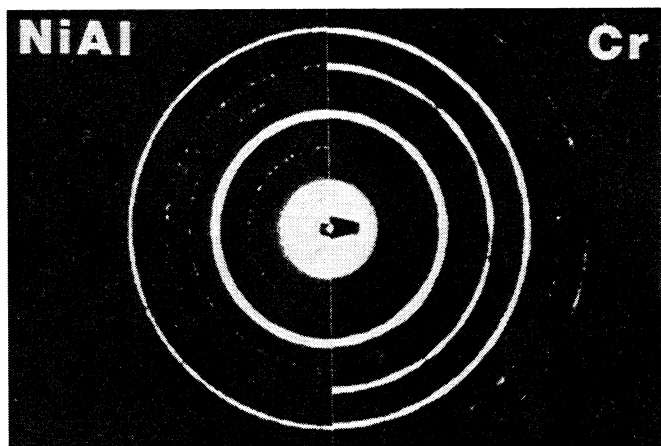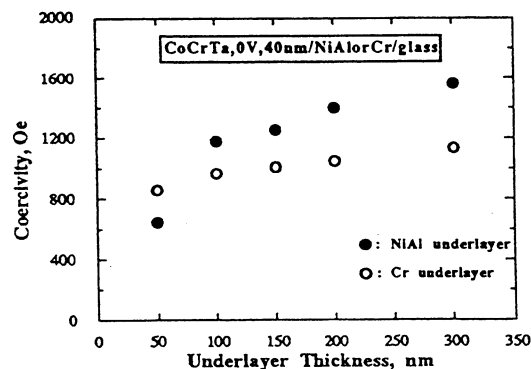
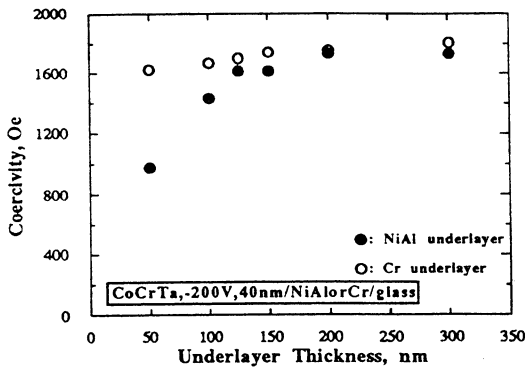Fig. 2. TEM diffraction ring patterns of 100nm NiAl and Cr.

Fig. 5. Coercivity vs. underlayer thickness of a 40nm CoCrTa film sputter-deposited with a -200V substrate bias. NiAl and Cr underlayers were deposited without bias.
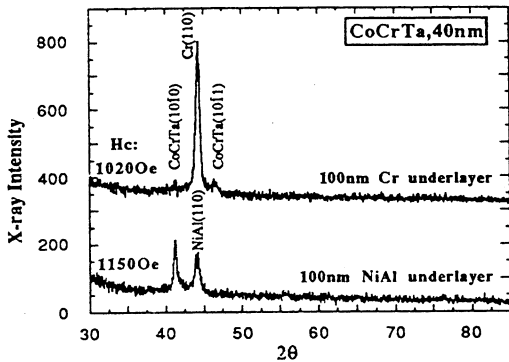

Fig. 6. X-ray diffraction spectra of CoCrTa/Cr and CoCrTa/NiAl films on glass substrates. All film layers were sputtered without substrate bias.
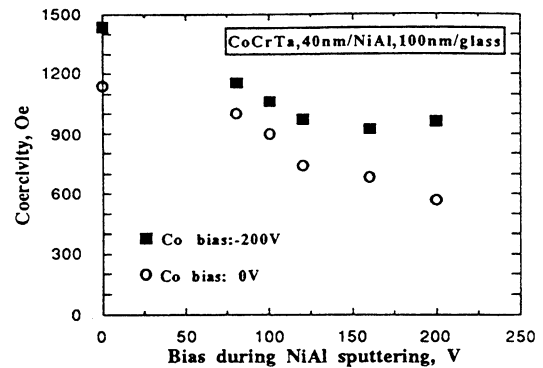

Fig. 7. Coercivity values of CoCrTa/NiAl films vs. voltage of substrate bias during the NiAl's deposition.

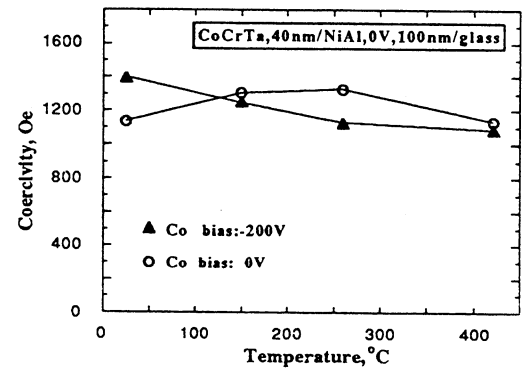Fig. 8. Coercivity values of CoCrTa/NiAl films vs. substrate temperature during the sputtering process.

increases slightly with heat when no bias is applied during CoCrTa deposition and actually decreases if bias is applied. However, it is well known that for Cr underlayers heat causes a Cr {002} texture to develop leading to a {11$\bar{2}$0} CoCrTa texture and the Hc to increase substantially. For our NiAl films, x-ray diffraction studies show that heat does not promote a {002} NiAl texture nor a {11$\bar{2}$0} CoCrTa texture. Furthermore, the {10$\bar{1}$0} texture tends to be degraded.

IV. CONCLUSIONS

The use of NiAl as an underlayer for Co alloy longitudinal recording media has been investigated for the first time. We found that the sputter-deposited NiAl films have a B2 ordered structure and a smaller grain size than Cr. The NiAl underlayers enhance the Co-alloy film's {10$\bar{1}$0} texture and increase their in-plane coercivity. Bias sputtering of the NiAl has been found to deplete the NiAl film of its Al content which deteriorates the B2 structure available for Co's epitaxial growth. It is anticipated that this Al content loss can be compensated for by adjusting the sputtering target composition. Substrate heating during deposition of the CoCrTa/NiAl is not as helpful as in the case of the CoCrTa/Cr because of the inability of the NiAl to develop {002} texture.

REFERENCES

[1] S. Iwasaki, K. Ouchi and N. Honda, IEEE Trans. Magn., vol. 16, 1111 (1987).
[2] D.J. Rogers, J.N. Chapman, J.P.C Bernards and S.B. Luitjens, IEEE Trans. Magn., 25, 4180 (1989).
[3] T. Yogi, C. Tsang, T.A. Nguyen, K. Ju, G.L. Gorman and G. Castillo, IEEE Trans. Magn., vol. 26, 2271 (1990).
[4] K. E. Johnson, Proceedings of the Second International Symposium on Magnetic Materials, Processes, and Devices of the Electrochemical Society, vol. 92-10, 27 (1991).
[5] T. Lin, and T. Yamashita, IEEE Trans. Magn., vol. 24, 2700 (1988).
[6] H. Suzuki, N. Tsumita, M. Hayashi, Y. Shiroishi and Y. Matsuda, IEEE Trans. Magn., vol. 26, 2280 (1990).
[7] Rajiv Ranjan, J. Appl. Phys., 67 (9), 4698 (1990).
[8] T. Kogure, S. Katayama and N. Ishii, J. Appl. Phys., 67 (9), 4701 (1990).
[9] R. Ranjan, J. Chang, T. Yamashita and T. Chen, J. Appl. Phys.,73 (10), 5542 (1993).
[10] T.A. Nguyen and J.K. Howard, J. Appl. Phys., 73 (10), 5579 (1993).
[11] N. Tani, M. Hashimoto, Y. Murata, M. Ishikawa, Y. Ota, and K. Nakamura, J. Appl. Phys., 67 (12), 7507 (1990).
[12] K. Hono, B. Wong and D.E. Laughlin, J. Appl. Phys., vol. 68, 4734 (1990).
[13] R.D. Noebe, R.R. Bowman and M.V. Nathal, International Materials Rev., vol. 38, No. 4, 193 (1993).
[14] JCPDS diffraction data card, JCPDS, 1601 Park Lane, Swarthmore, Pennsylvania.
[15] S.R. Butler, J.E. Hanlon and R.J. Wasilewski, J. Phys. Chem. Solids, vol. 30, 1929 (1969).
[16] S.L. Duan, J.O. Artman, B. Wong and D.E. Laughlin, J. Appl. Phys., 67 (9), 4913 (1990).
[17] Y. Deng, D.N. Lambeth, L.L. Lee and D.E. Laughlin, J. Appl. Phys., 73 (10), 6677 (1993).